Available online at www.sciencedirect.com
SCIENCE DIRECT®
Journal of Sound and Vibration 281 (2005) 763–782
JOURNAL OF SOUND AND VIBRATION
www.elsevier.com/locate/jsvi

Vibration transmission through a frame typical of timber-framed buildings

Robert J.M. Craik*, Laurent Galbrun

School of the Built Environment, Heriot-Watt University, Riccarton, Edinburgh EH14 4AS, UK

Received 3 July 2003; accepted 2 February 2004
Available online 29 September 2004

Abstract

A study of vibration transmission through a frame typical of timber-framed buildings was undertaken in order to establish whether or not statistical energy analysis (SEA) could be used to model such structures. Examination of individual beam junctions showed that the normal assumption that junctions are rigid was not valid and that the junctions were better modelled as pinned junctions (sometimes also called hinged junctions) through which no moments are transmitted. It was also found that there were significant fluctuations in the response due to the low modal overlap factor of the beams. When appropriate corrections for both the junction transmission and the low mode count were taken into consideration, there was satisfactory agreement between the measured and predicted results.

These theories were then used to model vibration transmission through a large two-storey timber frame and it was found that standard SEA models could be used to predict the mean response and that the fluctuations about that mean could also be estimated.

1. Introduction

Statistical energy analysis (SEA) has been used to predict and model sound and vibration transmission through masonry (concrete and brick) buildings for over 30 years. It can be used to predict the transmission between widely separated rooms in a building [1] and an international

*Corresponding author. Tel.: +44-1314495111; fax: +44-1314514617.
E-mail address: r.j.m.craik@hw.ac.uk (R.J.M. Craik).

0022-460X/$ - see front matter © 2004 Elsevier Ltd. All rights reserved.
doi:10.1016/j.jsv.2004.02.015

standard EN12354 [2] has recently been adopted for the calculation of flanking transmission in buildings which is based on a simplified version of SEA.

However, during the last 30 years the construction industry has changed direction and masonry buildings are far less common. Instead there has been a move towards lighter buildings of which timber-framed buildings are typical. In 2001, 60% of new houses built in Scotland and 6% of new houses in England were timber-framed [3]. These buildings consist of a timber frame with plasterboard, plywood or other sheet material attached to the frame. The buildings are usually much lighter making assembly simpler and components can often be manufactured rather than being assembled on site, leading to faster and cheaper construction.

High levels of sound insulation can be achieved in these buildings not by the addition of mass but by the careful use of multi-component walls and floors in which attenuation takes place at each of the junctions. Timber buildings have many such junctions and therefore there are many opportunities for improving sound transmission properties. However, a very good design can easily be compromised by poor construction techniques.

Previous attempts have been made to apply SEA to these types of buildings but with mixed success. There has been some success at using SEA to model airborne sound transmission through lightweight walls, notably by Craik and Smith [4,5]. The modelling of airborne sound transmission poses the simplest of all problems as airborne excitation ensures uniform excitation of the wall and therefore there is no significant lateral transmission from one sheet of plasterboard to another on the same side of the same wall. Attempts to model flanking transmission or impact sound insulation, where propagation across the surface of a wall or floor must be included, have been less successful. Flanking transmission has been studied by Nightingale and Bosmans [6,7] but their measured data is of limited value as there is no underlying theoretical model to provide a framework for interpreting the data and hence the data from their system cannot be generalised to other systems. There have also been other studies of sound transmission through timber-framed buildings but most studies not specifically attempting to model transmission theoretically suffer from the problem that key parameters are not measured. For example, there are many studies of airborne sound transmission through timber buildings, but if details of the construction (such as the number of nails) or details of the damping of the structure and the cavities are not given, then there will be insufficient data to provide robust predictions that can be compared with measured data (typically level difference).

In this paper sound transmission through a timber-framed building is studied by starting with a fundamental part of the problem, namely, examining the unclad timber frame in isolation. This requires an understanding of transmission at beam junctions.

One of the properties of beams is that it is not possible to have both a reverberant vibration field (which requires low damping) and a high modal overlap (which requires a high damping if the modal density is low) at the same time. In SEA it is commonly believed that both are required for successful modelling. This paper also addresses that perceived limitation.

The paper begins with a study of vibration transmission between two individual beams coupled in the same way as they would be in a real building. This study identified problems with defining junction transmission and how best to model it and also allowed examination of the problems associated with low mode count.

This is followed by a study of a large two-storey timber frame in which vibration transmission takes place over relatively long distances across many structural junctions.

2. Outline theory

As most of the beams in a building will meet at right angles, the simplest and most general beam junction consists of six beams meeting at a single point as shown in Fig. 1. Each of the six beams will support bending waves in two planes, plus torsional waves and longitudinal waves and would therefore be modelled as four SEA subsystems. In addition there will be two bending nearfield waves which are not modelled as subsystems as they are associated with motion that only occurs next to junctions (or sources). Vibration transmission across this type of junction can be calculated using a wave approach in which a wave of one type is assumed incident on the junction and given the requirement of continuity and equilibrium, the waves on the other beams can be calculated. This allows the transmission coefficient to be calculated for the junction, from which the coupling loss factor can be computed.

The method adopted for calculating the wave transmission coefficient is well described in literature [1,8] and is therefore not given in detail here. However, within the general method there are different assumptions that can be made about the conditions at the boundary which therefore need to be specified.

2.1. Rigid junction

The simplest junction is where all the beams are assumed to be rigidly connected together. In such a junction (shown in Fig. 2 for two beams only) any displacement (in the x, y or z directions) of one beam must be matched by equal displacement in that direction of all beams at the joint. This satisfies continuity of displacement. Similarly, if there is rotation about any axis of one beam then there must be an identical rotation in all other beams, giving continuity of slope or rotation. Finally for the junction as a whole, there must be equilibrium of forces in all directions and

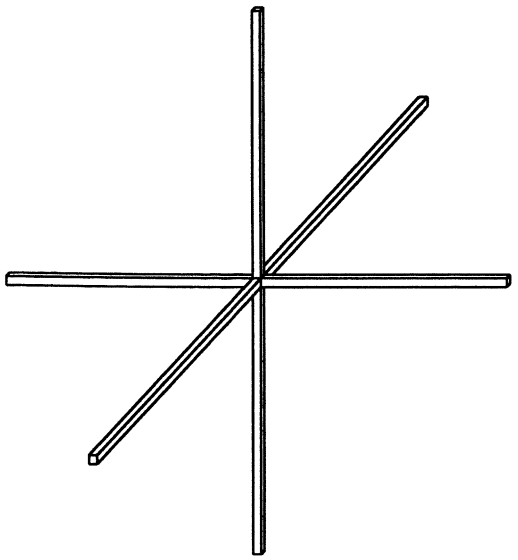

Fig. 1. Idealised junction showing the intersection of 6 beams at a point.

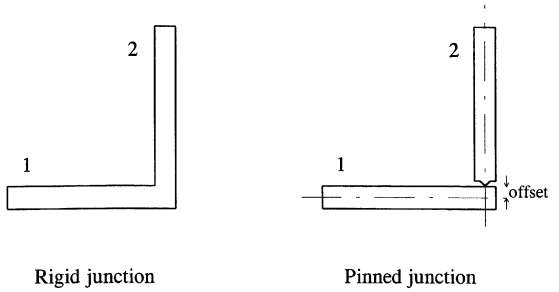

Fig. 2. Idealised rigid and pinned two beam junction.

moments about all axes. Together these requirements allow 36 equations to be written for a six beam junction, which can be solved to give the displacements of the six waves on each beam (two bending, two bending nearfield, one longitudinal and one torsional). For a junction with N beams, a set of $6N$ equations needs to be solved.

2.2. Pinned junction

During the study it was found that many real junctions in which the beams are nailed or screwed together did not behave as rigid junctions. In this case a better model was found, which assumes that the beams are pinned together. This is also shown for the simple case of two beams in Fig. 2.

If one beam that forms part of a two beam junction is moved, then it has been found that the beam can be rotated with little or no rotation of the other beam. This is because there is weak transmission of moments. In an extreme case there will be no moment transmitted across the junction (about any axis) and the junction is then pinned (or hinged). There is still continuity of displacement so that the beams move together but there is no continuity of slope. The rotation of the pinned beam is independent of the rest of the junction.

The equilibrium of the forces (for the junction as a whole) is unchanged but the equations describing equilibrium of the moments change. As no moments are transmitted to each pinned beam, there must be equilibrium of the moments (about each axis) for each individual pinned beam as well as equilibrium for the junction as a whole. The moment equilibrium conditions for each pinned beam replace the continuity of slope condition for a rigidly connected beam. The overall equilibrium of moments remains unchanged.

In practise it is relatively straightforward to set up the equations so that each beam is either rigidly attached to the junction (in which case there is continuity of slope and a contribution to the overall moment equations) or the beam is pinned (in which case nothing can be said about the slope but equations can be written for the equilibrium of moments for that beam).

The simplest approach is to have a junction point where the beams meet and to which other beams are attached. If the pinned point is at the intersection of the centre lines of the beams then it can be shown [9] that a bending wave on one beam will not transmit a moment to the other beam and therefore there will be no transmitted bending wave. However, in real junctions the pinned point of connection is usually offset from the intersection of the centre lines of the beams and this offset should be included. In the example in Fig. 2, the point of connection is offset from the

centre line of beam 1. Shear forces acting on the connection point then generate moments so that bending waves are transmitted.

In some junctions the beams are arranged so that there is not a single intersection point but two or more such points. A simple example is shown in Fig. 3. Beams 1 and 2 (in Fig. 3) are rigidly connected together as are beams 3 and 4. Each pair of beams is then pinned to the other pair. If a single junction point is assumed then beams 1 and 2 could be rigidly attached to this point, but if beams 3 and 4 are pinned then they are not modelled correctly. The correct way to model this would be to have several intersection points to which each beam is either rigidly or flexibly attached, with each intersection point then rigidly or flexibly attached to the other intersection points.

In building structures there are often complex junctions but the layout of the timber frame members and the position of the nails would not normally be known and so an accurate model of each joint cannot be produced. Therefore, more complex models involving more than one intersection point cannot at this stage be justified. Examples of junctions like the one in Fig. 3 exist in the frame structure examined later. It was found that different modelling strategies (such as making 1 and 2 rigid and 3 and 4 pinned or vice versa) had little effect on overall transmission.

2.3. Calculating the coupling loss factor

Whichever model is used (rigid or pinned) the results will be a set of transmission coefficients giving the ratio of power transmitted to the power incident on the junction. It should be noted that the transmitted wave may be of a different type to the incident wave.

The coupling loss factor between any two subsystems 1 and 2, η_{12}, required by the SEA model is then given by [1]

$$\eta_{12} = \frac{c_{g1}\tau_{12}}{4\pi f L_1}, \tag{1}$$

where L is the length of the beam, τ is the transmission coefficient and c_g is the group velocity of the incident wave. For bending waves, the group velocity is twice the phase velocity and for longitudinal and torsional waves, it is equal to the phase velocity.

2.4. Low-frequency correction

When using SEA it is assumed that the response of each subsystem is determined by resonant modes. This leads to two requirements for an SEA subsystem. The first is a minimum number of modes in each frequency band, the mode count, necessary for statistical averaging over modes to

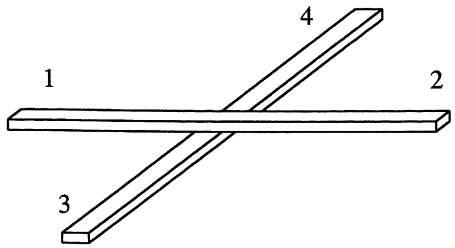

Fig. 3. Two continuous beams connected together.

be meaningful. The mode count, N, is the product of the bandwidth, Δf, and the modal density, n. The modal density is [1]

$$n = \frac{2L}{c_g}. \tag{2}$$

The second requirement is that the bandwidth of each mode should be greater than the average spacing between them, so that there are not parts of the spectrum where the response is not determined by resonant modes. This ratio, M, is known as the modal overlap factor and is given by

$$M = f\eta n, \tag{3}$$

where η is the total loss factor.

The minimum number of modes per band depends on the system being studied but clearly there needs to be at least one mode per band. Similarly, it has been found that a modal overlap of less than unity leads to large fluctuations in response (as a function of frequency) and that there is a tendency for the coupling between subsystems to be reduced [10].

An example of the bending mode count and modal overlap for a $2.5 \times 0.1 \times 0.05$ m timber beam (length $\times$ depth $\times$ width) is given in Fig. 4. It can be seen that the bending mode count only exceeds unity above 2000 Hz and that the modal overlap never exceeds unity.

Two curves are shown for the modal overlap factor. The upper curve is based on a value of total loss factor (TLF) which is the internal loss factor plus the sum of the standard SEA coupling loss factors for the two connected beams described later (the second beam was 2.0 m long). The lower value is based on an uncoupled beam where the TLF is equal to the internal loss factor which in this case is 0.01 (the measured value averaged over frequency). This is the lower limit to the modal overlap factor and is important in the discussion on confidence limits.

A method for correcting the coupling loss factor between subsystems, to account for the low modal density and low modal overlap factor, was proposed by Craik et al. [11]

$$\eta_{12} = \eta_{12\infty} \frac{\mathrm{Re}(Y_2)}{\mathrm{Re}(Y_{2\infty})}, \tag{4}$$

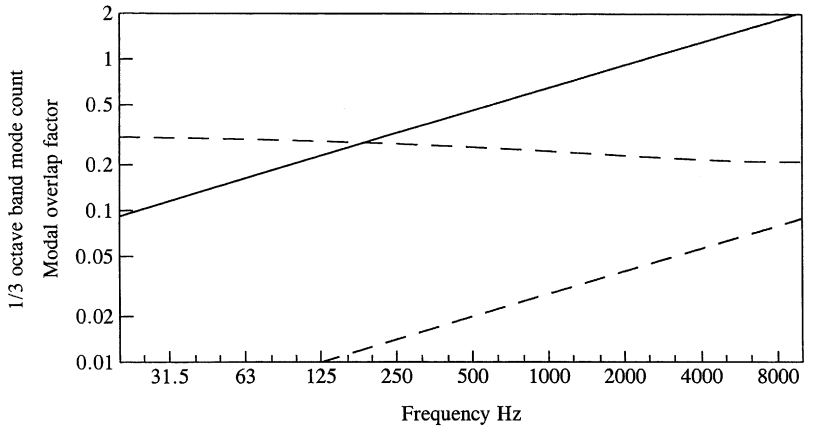

Fig. 4. Predicted $\frac{1}{3}$ octave band mode count and modal overlap for a 2.5 m long timber beam: ——, mode count; - - - - , modal overlap (upper curve computed from TLF and the lower from ILF).

where η_{12} is the actual coupling loss factor, $\eta_{12\infty}$ is the standard CLF usually calculated from infinitely extended subsystems, Y_2 is the mobility of the receiving subsystem and $Y_{2\infty}$ is the mobility of the receiving subsystem assuming it to be infinitely extended. This equation can be used at all frequencies as $\mathrm{Re}(Y_2)/\mathrm{Re}(Y_{2\infty})$ tends to unity as the frequency increases.

The point mobility for an infinite beam excited at the centre is [9]

$$\mathrm{Re}(Y_\infty) = \frac{1}{2\rho_l c_g}, \tag{5}$$

where ρ_l is the mass per unit length (kg/m).

The actual mobility can be determined by summing the contribution of each of the individual modes [1]

$$\mathrm{Re}(Y_2) = \sum_n \frac{1}{2\pi f_n m\eta[1 + (f/f_n - f_n/f)^2/\eta^2]}, \tag{6}$$

where f_n is the nth resonant frequency, m is the subsystem mass, and η is the damping (total loss factor). This approach gives the spatially averaged mobility for each mode so there is no position variable and, as with all SEA calculations, all modes are assumed to be equally excited so there is equal weighting for all modes.

Simple estimates of the resonance frequencies can be found in standard texts [1,9] for beams with idealised boundary conditions. However, a wide variety of junctions can exist which are far from idealised and so a more accurate estimate of the resonance frequencies can be made by including the phase change, ϕ, that occurs when a wave is reflected at each end. A beam resonance will occur if a wave closes on itself in phase. This happens when the total phase change due to propagation along the beam and the reflections is a multiple of 2π giving [9],

$$2kL - \phi_1 - \phi_2 = 2n\pi, \tag{7}$$

where k is the wavenumber, $\phi_{1,2}$ is the phase change at each end and $2kL$ is the phase change as a wave travels a distance $2L$.

The phase change at each end can be obtained directly from the model for calculating the transmission coefficients and is found from the complex amplitude of the reflected wave at the beam end being considered. Usually ϕ lies in the range $-\pi$ to $-\pi/2$.

For bending waves, where the wavespeed is a function of frequency, the resonance frequencies are given by

$$f_{nB} = \sqrt{\frac{B}{\rho_l}}\frac{\pi}{2}\frac{(n+\phi')^2}{L^2}, \tag{8}$$

where B is the bending stiffness and $\phi' = (\phi_1 + \phi_2)/2\pi$. It should be noted that this equation assumes that bending nearfield waves generated at one end have no influence at the other end. This interaction can be important for the first resonance but is negligible above the second resonance [9]. For longitudinal and torsional modes where the wavespeed, c, is independent of frequency the resonance frequencies are given by

$$f_{nL,T} = \frac{c_{L,T}}{2}\frac{(n+\phi')}{L}. \tag{9}$$

In both Eqs. (8) and (9) n is an integer $(1, 2, 3 \ldots)$ where the lowest value is found from the requirement that $n > -\phi'$ (typically n starts at 1).

The use of Eq. (4) to calculate the revised CLF will give results like those shown in Fig. 5. This gives the CLF between two beams and was used to calculate the level difference shown in Fig. 8. The peaks occur at the resonance frequencies in the receiving subsystem and the dips occur between these resonances.

When all the CLFs are corrected (using Eq. (4)) the change in CLF will in turn change the TLF for each subsystem. These revised values for the TLF can then be used to compute revised values for the CLF and so on. Final values can be found through a process of iteration with typically 5–10 iterations being required. The change in the CLF after the 1st and 10th iteration are both shown in Fig. 5. Repeated iterations will generally lead to larger fluctuations.

The upper and lower limits for the mobility ratio and hence the CLF can be found from an analysis of the mobility. The maximum value occurs by setting $f = f_0$ in Eq. (6) giving the upper limit as [1]

$$\text{Upper limit} = 10 \log \frac{2}{\pi f \eta n}. \tag{10}$$

The minimum value occurs approximately midway between two resonances and can be given by [1]

$$\text{Lower limit} = 10 \log \frac{4 f \eta n}{\pi}. \tag{11}$$

The upper and lower limits to the CLF can then be found from Eqs. (10) and (11), respectively and these are also shown in Fig. 5. The correction made in the first iteration is well defined and so the upper and lower limits can be accurately predicted. It is interesting to note that the limits increase with frequency as the modal overlap (shown in Fig. 4) decreases with frequency.

After repeated iterations the extent of the fluctuations depends on the properties of the system and in particular on the complex interaction between the TLFs and the CLFs. In the limit the

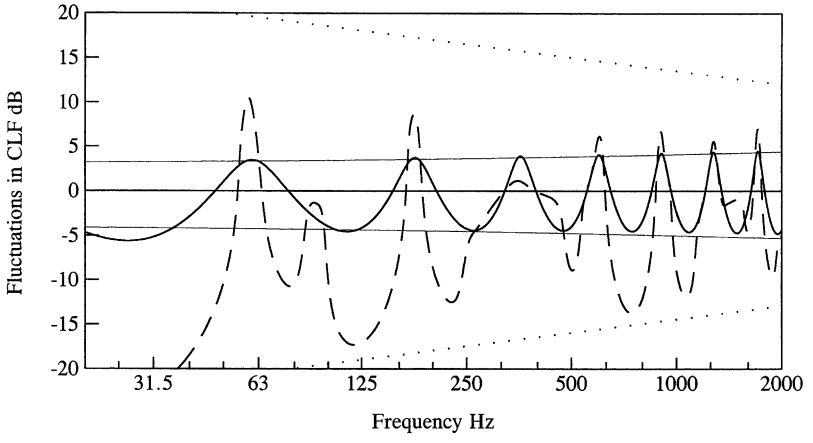

Fig. 5. Fluctuations in the coupling between two beams: ——, 1 iteration; - - - - -, 10 iterations; ———, limits based on SEA TLF; ……, limits based on ILF = 0.01.

TLF cannot go lower than the ILF and this then places a lower limit on the TLF and hence a limit on the fluctuations. Those limits are also shown in Fig. 5 and decrease with frequency as the modal overlap increases with frequency (shown in Fig. 4). It can be seen that these limits (shown by the dotted line) are reasonable for the lower limit but are very conservative for the upper limit.

Measurements are usually carried out in $\frac{1}{3}$ octave bands and this frequency averaging will tend to reduce the magnitude of the fluctuations that occur with frequency. The peak values are generally less than $\frac{1}{3}$ octave wide and therefore band averaging will result in a much lower peak. If the modal bandwidth is less than the measuring band then the band average is effectively an average across the entire frequency range (for that mode). This gives the band averaged upper limit as [1]

$$\text{Upper band limit} = 10 \log \frac{1}{N} \tag{12}$$

for frequencies where $N < 1$.

The dips in the curves in Fig. 5 are relatively wide and so band averaging will have a relatively small effect. Eq. (11) therefore provides a realistic conservative estimate of the lower limit in the region where the modes are widely spaced. Eqs. (11) and (12) are clearly not valid if $N > 1$.

3. Two coupled beam experiments

The first experiments were carried out on two coupled beams connected as shown in Fig. 6. Each beam was 100×50 mm in cross-section and the beams were 2.0 and 2.4 m long with the properties given in Table 1. All values in the table are based on measured data except Poisson's ratio for which a value of 0.3 was assumed. Young's modulus was measured in the axial direction and the damping value was the measured value averaged across all frequencies. Initially the two beams were screwed together in the usual manner, as shown in Fig. 6(a). However, as it was found that this junction did not behave as a rigid junction, a second version was constructed in which plywood reinforcing plates were screwed and glued on each side of the junction as shown in Fig. 6(b). This junction behaved as a rigid junction.

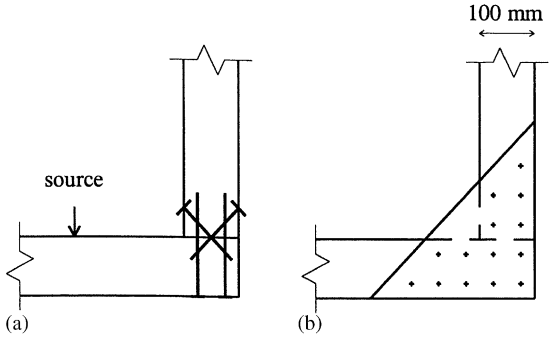

Fig. 6. Two beams connected at right angles: (a) screwed junction; (b) reinforced junction.

Table 1
Material properties and dimensions of the structures examined (Young's modulus measured in the axial direction)

Structure	Dimensions (m)	Density (kg/m^3)	Young's modulus ($\times 10^9$ N/m^2)	Poisson's ratio	Damping (ILF)
2 coupled beams	$2.0 \times 0.1 \times 0.05$ (source)	480	9.0	0.3	0.01
	$2.4 \times 0.1 \times 0.05$ (receiver)	480	9.0	0.3	0.01
Large timber frame (22 beams)	$4.8 \times 0.088 \times 0.038$ (11 beams)	480	9.0	0.3	0.01
	$2.3 \times 0.088 \times 0.038$ (5 beams)	480	9.0	0.3	0.01
	$2.4 \times 0.088 \times 0.038$ (4 beams)	480	9.0	0.3	0.01
	$2.5 \times 0.088 \times 0.038$ (2 beams)	480	9.0	0.3	0.01

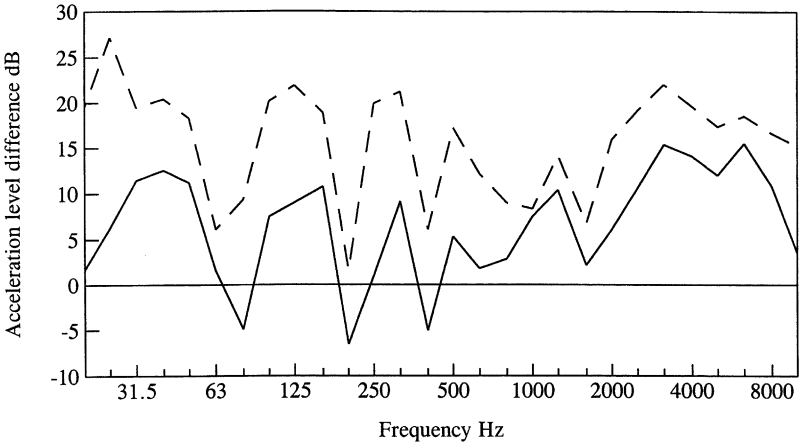

Fig. 7. Measured level difference between two beams: ——— , rigidly connected beams; - - - - - , real screwed connection.

Vibration measurements were carried out by exciting the 2.0 m beam with an impact hammer, moving the source along the beam between hammer hits. The space-averaged acceleration of each beam was then measured from which the vibration level difference could be computed.

The vibration level difference that was measured for each of the two cases can be seen in Fig. 7. It can be seen that there is a considerable difference between the two sets of results. The rigid beam has an average level difference of about 5 dB whereas the real junction has an average value of about 15 dB.

A comparison between the measured and predicted level difference (measured and computed in 1/24th octave bands) for the rigid joint can be seen in Fig. 8. A correction has been made to the CLFs to account for the low number of modes as described above (CLF correction made in 10 iterations). It can be seen that there is good agreement between the measured and predicted level difference. The position of the dips in the level difference is due to the modal frequencies in the receiving subsystem. The frequencies at which the dips appear are similar to the frequencies predicted and the differences can probably be attributed to the uncertainties in the beam length

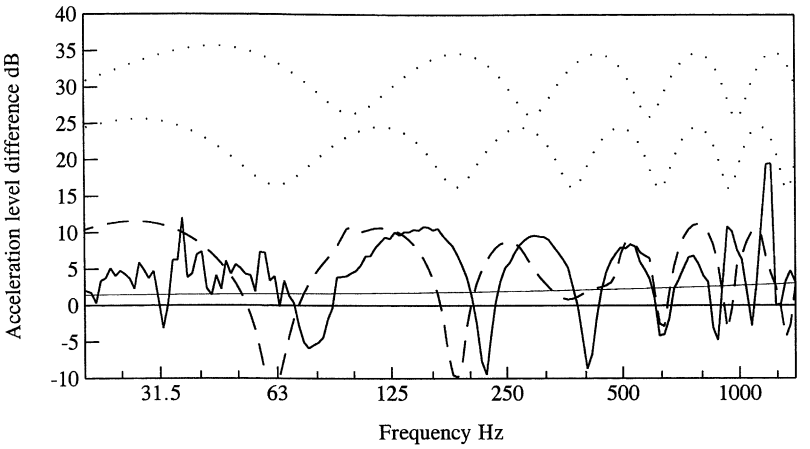

Fig. 8. Measured and predicted level difference between two rigidly connected beams: ▬▬, measured; ——— , SEA mean; - - - - - , predicted with low-frequency correction; ⋯⋯, predicted beam mobility (upper is source beam and lower is receiving beam).

(the physical beam lengths are 2.0 and 2.4 m but the subsystem lengths are 1.95 and 2.45 m measured to the intersection of the centre lines), the influence of the reinforcing plates and uncertainties in the material properties. The magnitude of the level difference is also correct.

The upper part of the figure gives the ratios $\mathrm{Re}(Y_{2\infty})/\mathrm{Re}(Y_2)$ and $\mathrm{Re}(Y_{1\infty})/\mathrm{Re}(Y_1)$ for comparison. The ratio is the inverse of Eq. (4) as it is the level difference that is being displayed and not the CLF. It can be seen that the dips in the receiving subsystem mobility correspond to the dips in the level difference and that the fluctuations of the source subsystem mobility have almost no effect.

The mobility ratios were computed using the first SEA estimate of the TLF. Updating the TLF to reflect the change in CLF, etc. increases the magnitude of the difference between the peaks and dips in the mobility ratios from about 10 up to 20 dB as was shown in Fig. 5. However, the fluctuations in the level difference are not as large as the fluctuations in the CLF since there are also fluctuations in the TLF. Thus at around 40 Hz the CLF, η_{12}, is about 20 dB less than the SEA mean (see Fig. 5) but the TLF is also smaller and so the overall level difference is not 20 dB from the SEA mean but is about 10 dB.

The measured level difference for the real joint (Fig. 6(a)) is shown in Fig. 9 together with two different theories. In each case a correction has been made to account for the fluctuations associated with low modal density and band averaging has been carried out over the predicted narrow band response. The lower predicted curve corresponds to the rigid joint and is the same result as was shown in Fig. 8, except that the data has been converted to $\frac{1}{3}$ octave band data. The upper curve corresponds to a transmission model where the joint is assumed to be pinned at a point which is offset from the centre line of beam 1 (see Fig. 2).

It can be seen that up to about 2 kHz the measured result lies close to the pinned joint result although, as with the rigid case, the peaks and dips do not occur at the correct frequencies. However, the measured and (pinned) predicted results have the same mean value and fluctuations of the same magnitude. This suggests that the pinned joint theory is sufficient to give the

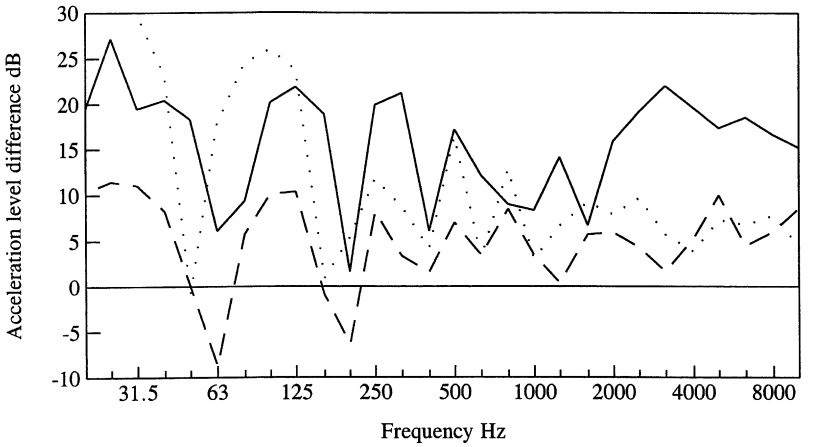

Fig. 9. Measured and predicted level difference between two beams screwed in the normal manner: ——— , measured; - - - - - , predicted for a rigid joint; ·····, predicted for a pinned joint.

magnitude of transmission and, hence, the mean value and the extent of the fluctuations, but that the phase of the reflected wave is not sufficiently accurate to enable the exact frequency of the dips to be predicted. This is sufficient for SEA models where it is always assumed that modal frequencies cannot be predicted with certainty.

Above 2 kHz the measured data shows much larger level difference than is predicted by either model. This appears to be a general conclusion as can be seen in many of the results presented in later sections though there is no obvious reason why this should occur.

A number of other junctions have been tested and in general, unless special precautions are taken to ensure rigidity of the junction, then the results are closer to the pinned junction model.

It should be possible to devise an experiment which would allow the equivalent stiffness for the nail/screw to be determined and to include this in the transmission model. However, such refinements to the model are impractical. Both the model and the equivalent stiffness would vary depending on how many nails or screws are present and how they are attached. Such detailed knowledge will almost never be known and therefore it is better to accept a small error and keep the model simple.

4. Large-scale laboratory experiments

In order to test these theories on more realistic structures, a large frame structure was constructed as shown in Fig. 10. The frame was 4.9 m high and corresponds to a full size double storey building. The frame members were all 88 × 38 mm with the properties given in Table 1. All beams were nailed/screwed in the usual manner (Fig. 6(a)).

When predicting transmission at each joint, it was assumed that the notional centre of each joint was at the centre of the upright beams and that these were rigidly connected together (as they are a single piece of wood). The other beams were then assumed to be connected by pinned connections offset by an appropriate amount. This approach means that a single general model

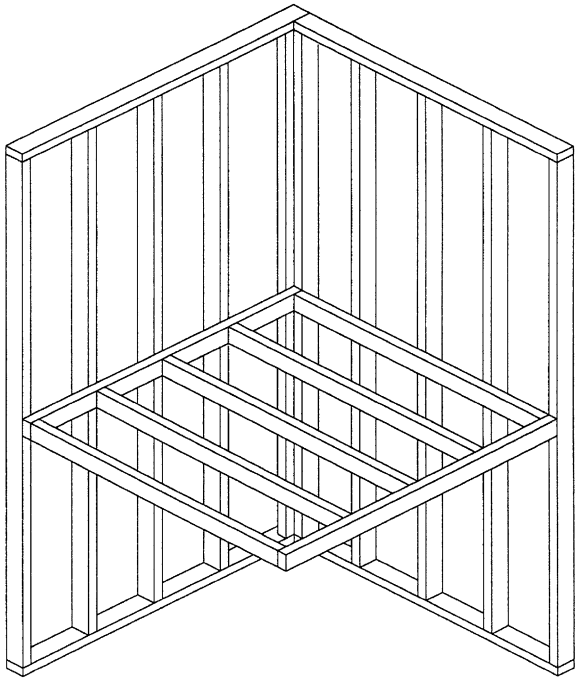

Fig. 10. Two storey timber frame 4.9 m overall height and 2.4 m each side.

can be used to model any junction but means that if there are two continuous beams connected together, then only one of them can be modelled as continuous (see discussion for Fig. 3). Alternative modelling approaches were used and all gave similar overall results.

The measured and predicted vibration level difference for transmission between two adjacent beams is given in Fig. 11. This requires transmission across at least two structural junctions. The measured level difference exhibits fluctuations that are not unlike that of the two beam system. The fluctuations are discussed in the next section. The standard SEA prediction passes approximately through the middle of these results.

Similar results can be seen in Fig. 12 for transmission over a longer distance to another of the long beams. Again the SEA prediction passes through the measured results.

If each junction is taken as the boundary of a subsystem then many of the beams will be very short. There are many such short subsystems in the frame, even though most of them are constructed from a single long piece of wood. These subsystems are typically 600 mm long in this frame and would normally be too short to be modelled as subsystems. However, if the SEA model is to be simple then there is no realistic alternative modelling approach. In junctions between plates, very small elements can be modelled as plate elements within a larger joint and then be modelled exactly [12]. However, adopting this approach in the timber frame would result in each short beam being an internal component in a large junction rather than being the connecting element between junctions. The entire frame would then be modelled with three joints (one along the top, one in the middle and one along the bottom). Such a modelling approach is effectively a deterministic model and therefore loses all the advantages of SEA.

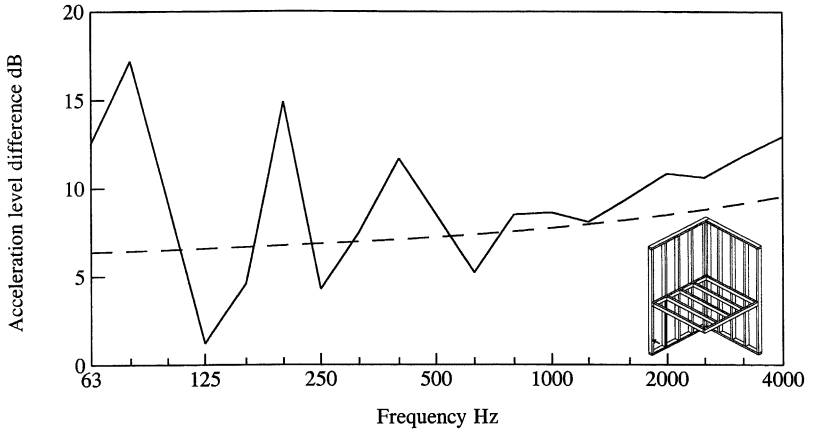

Fig. 11. Measured and predicted transmission between two beams in a large frame over a minimum of 2 structural junctions: ——— , measured; - - - - - , predicted; ←, source; |, receiving subsystem.

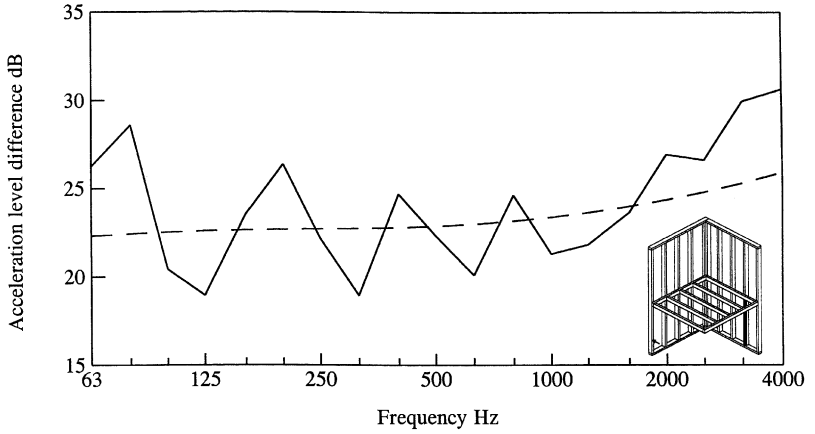

Fig. 12. Measured and predicted transmission between two beams in a large frame over a minimum of 7 structural junctions: ——— , measured; - - - - - , predicted; ←, source; |, receiving subsystem.

In the SEA model all the small elements were therefore included as SEA subsystems, even though the modal density and modal overlap are very small. The vibration of these subsystems was also measured and two examples are shown in Figs. 13 and 14 for transmission over a short and long distance, respectively. Perhaps surprisingly the results are reasonably good.

4.1. Establishing confidence limits

So far it has been shown that the standard SEA model can be used to predict the mean response of the beams that make up the frame. However, there are significant fluctuations about the SEA

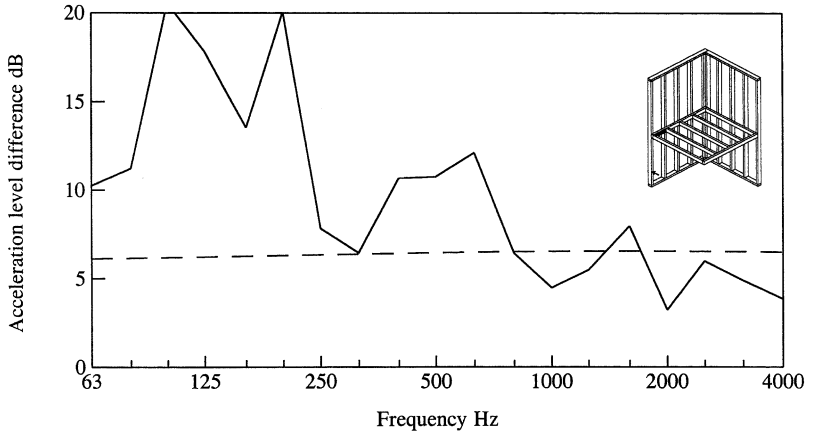

Fig. 13. Measured and predicted transmission to a small beam in a large frame over 1 junction: ——— , measured; - - - - - , predicted; ←, source; |, receiving subsystem.

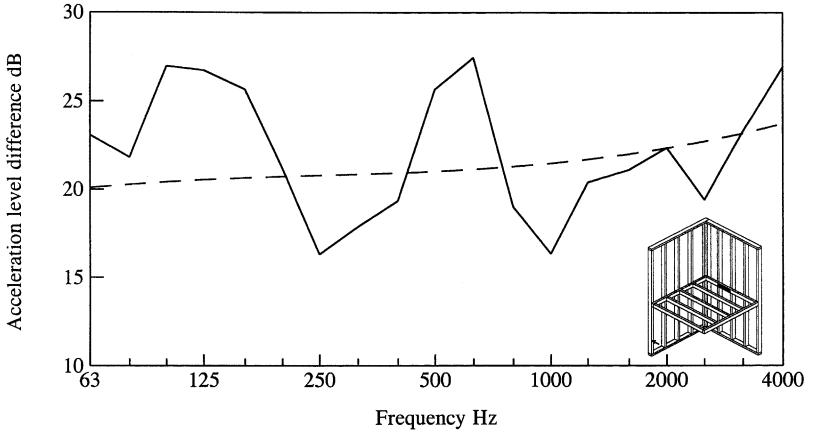

Fig. 14. Measured and predicted transmission to a small beam in a large frame over a minimum of 6 structural junctions: ——— , measured; - - - - - , predicted; ←, source; |, receiving subsystem.

mean which, as was shown in the two beam system, are due to the influence of the individual modes in the beams. Due to the uncertainties in the phase change at the boundaries, the exact frequency of the peaks and dips cannot be determined but it would still be useful if the overall magnitude of the fluctuations could be found. This section looks at ways of establishing the extent of these fluctuations.

One approach is to make a correction to each CLF (and then TLF and CLF and so on) as was done to give the results of Figs. 8 and 9. However, in the SEA model all the beams are assumed to have the same material properties and there are only a few different dimensions. This leads to the correction terms being the same for many of the CLFs. These corrections then become magnified and very large and unrealistic values are obtained.

In real structures (including this one) there are significant variations from one piece of timber to another and each junction will be slightly different. Therefore an alternative method of estimating the fluctuations is to assume that there is considerable randomness in the structure.

The velocity level difference, D, between two beams due to transmission along a specific path can be written as [1]

$$D_{1n} = 10 \log \frac{\eta_2 \eta_3 \eta_4 \cdots \eta_n m_n}{\eta_{12} \eta_{23} \eta_{34} \cdots \eta_{(n-1)n} m_1}. \tag{13}$$

If the correction for each CLF is assumed to be different (either because the subsystem is different or due to randomness in the system) then the corrections will sometimes be positive and sometimes negative and they will on average cancel out leaving the original SEA prediction. This is particularly true if there are many transmission paths included in the averaging process.

However, all transmission paths to the receiving subsystem n, end with coupling to subsystem n and therefore have the correction $\mathrm{Re}(Y_n)/\mathrm{Re}(Y_{n\infty})$. This correction is not averaged out as it is always present. Therefore an estimate of the upper and lower limit can be found by considering the mobility ratio of the receiving subsystem (which is the correction for all CLFs to subsystem n).

This mobility ratio in turn requires knowledge of the damping of subsystem n and is itself affected by fluctuations of the CLFs. It was shown in Fig. 4 that conservative estimates of the modal overlap factor can be made by assuming the lowest value of TLF is the internal loss factor. This lower limit of TLF then gives a lower limit of modal overlap factor, a lower limit to the CLF and an upper limit to the level difference. In the same way the band-averaged peak mobility can be approximated by Eq. (12). As this is independent of the TLF, it is not affected by the iteration process involved in the calculation of TLF and CLF. The upper limit to the modal overlap gives an upper limit to the CLF and a lower limit to the level difference.

A comparison of these limits can be seen in Figs. 15–18. Fig. 15 shows the results for all 15 of the long vertical beams (2.4 m long) excluding the corner beams. The source is always horizontal as if it was exciting a wall (same as Fig. 11). The response is also horizontal as if the response of a wall. The fluctuations shown are the actual measured level difference minus the level difference predicted from a standard SEA model as was shown in Figs. 11 and 12. These fluctuations about the standard SEA model are compared with the predicted limits given by Eqs. (11) and (12). It can be seen that up to about 2 kHz the results fluctuate about zero so that the SEA model gives the correct average. Above about 2 kHz the measured level difference is higher than predicted as was also found in Fig. 9. It can also be seen that the limits obtained from Eq. (11) with a TLF of 0.01 and Eq. (12) give a good estimation of the upper and lower limits to the fluctuations about the SEA mean.

Similar results can be seen in Fig. 16 for 12 results measured on all the short beams (600 mm long) at the "floor" level. The source was the same as for Fig. 15 and the response was bending vibration in the horizontal plane. Note that the short beams are parts of a large single piece of wood. At the "floor" level there are four pieces of timber at the edge, three of which are modelled as four elements, each element being four subsystems (two bending, one longitudinal and one transverse). The limits are larger as the modal density is lower and the SEA model is probably less appropriate. Again the results vary about the zero line showing that the SEA model is a good

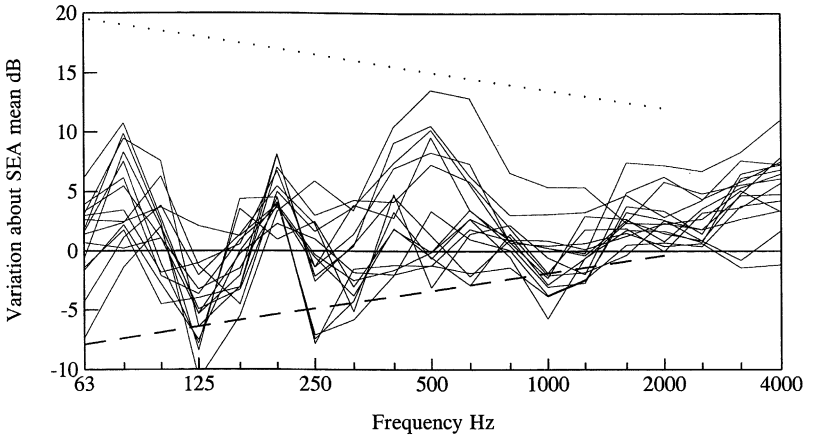

Fig. 15. Measured minus predicted level difference for transmission to 15 long vertical beams: ——— , measured; ·····, predicted upper limit from Eq. (11) (with $\eta = 0.01$); - - - - - , predicted lower limit from Eq. (12).

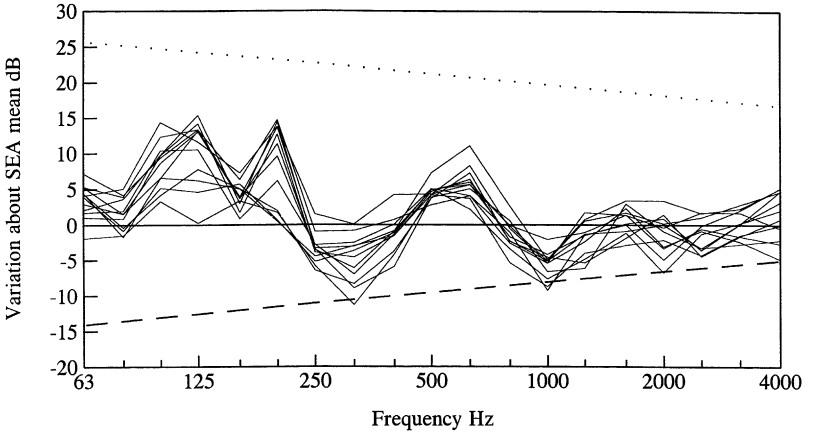

Fig. 16. Measured minus predicted level difference for transmission to 12 small beams at "floor" level: ——— , measured; ·····, predicted upper limit from Eq. (11) (with $\eta = 0.01$); - - - - - , predicted lower limit from Eq. (12).

estimator of the average and the results lie within the conservative limits. Although there is a large variation about the mean there is surprisingly little variation between the results.

In both Figs. 15 and 16 there are results for transmission over both short and long distances. There is no trend in these results with the variation being no better or worse as the distance increases.

One of the results of the tests on the two beams at right angles was that there was a significant difference between the model in which joints were assumed to be rigid and one where the beams were assumed to be pinned. Calculations show that the difference between the models is only significant for transmission through a right angle (as opposed to inline transmission). Measurements were therefore made from each of the four vertical "ground floor" beams (excited

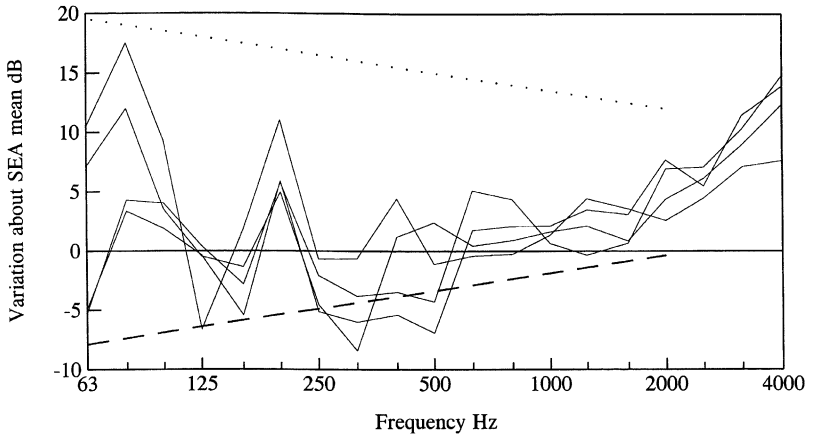

Fig. 17. Measured minus predicted level difference for transmission to four large beams at right angles to the source across a single pinned junction: ——— , measured; ·····, predicted upper limit from Eq. (11) (with $\eta = 0.01$); - - - - - , predicted lower limit from Eq. (12).

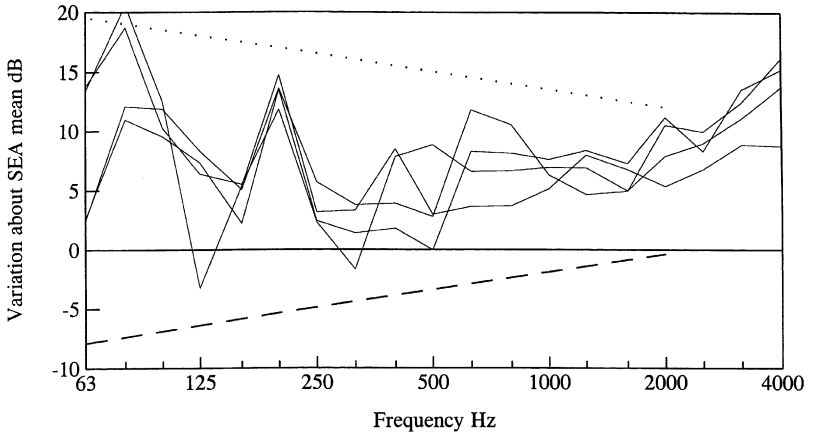

Fig. 18. Measured minus predicted level difference for transmission to four large beams at right angles to the source across a single rigid junction: ——— , measured; ·····, predicted upper limit from Eq. (11) (with $\eta = 0.01$); - - - - - , predicted lower limit from Eq. (12).

as if part of a wall) to the corresponding horizontal beams to which they are connected (with the response measured vertically as if part of a floor). The measured minus predicted level difference is shown in Fig. 17 for a model where the horizontal beam was pinned to the vertical beam and in Fig. 18 where it is rigidly connected.

It can be seen that in Fig. 17 the results fluctuate about the SEA mean and are well within the limits and similar to the results of Fig. 15. In contrast the results in Fig. 18 are consistently above the SEA mean (the zero line) by 5–10 dB. This confirms that it is more appropriate to model the junctions as pinned rather than rigid junctions.

5. Conclusions

The results of this paper allow a number of important conclusions to be drawn of particular importance to vibration transmission in timber-framed structures but also of general importance to SEA.

It has been found that the junction between timber beams does not behave as a rigid junction and is better modelled as pinned. Beams are only weakly coupled across junctions, so that there is a significant reduction in coupling. This improved approach to modelling has been confirmed in a full sized laboratory model.

Detailed measurements were made in a large frame structure. A common view of such structures is that they cannot be properly modelled using SEA as it is not possible to have both a reverberant vibration field (which requires low damping) and a high modal overlap (which requires a high damping if the modal density is low). Inevitably in such networks there are large fluctuations in the mobility of the components leading to large fluctuations in response (as a function of frequency). However, it was found that although the fluctuations can be large, they occur about the SEA mean value (as SEA theory predicts) and therefore the standard SEA model can be used to give the mean coupling and mean response.

Furthermore, the fluctuations in response can be related to the variations in the mobility of the subsystems. For this beam network (and for most beam networks) considerable randomness would be expected and therefore many of the causes of the fluctuations will cancel. This allows the fluctuation in response to be well estimated by the fluctuations in the mobility of the receiving subsystem. This conclusion is the same as that found for transmission between plates [11] and suggests that the application of the original finding is more general than was originally thought.

One of the limitations of SEA has always been the difficulty in predicting the fluctuations about the mean. The results of this paper show how details of the fluctuations can be determined for laboratory situations (like Fig. 8) and how limiting bands can be determined for field results (like Fig. 15).

References

[1] R.J.M. Craik, *Sound Transmission Through Buildings Using Statistical Energy Analysis*, Gower, London, 1996.
[2] BS EN 12354. Estimation of acoustic performance of buildings from the performance of elements, British Standard Institution, 2000.
[3] Timber Frame Industry Association, Statistics 2000/2001, 2001.
[4] R.J.M. Craik, R.S. Smith, Sound transmission through double leaf lightweight partitions—part I: airborne sound, *Applied Acoustics* 61 (2000) 223–245.
[5] R.J.M. Craik, R.S. Smith, Sound transmission through lightweight parallel plates—part II: structure-borne sound, *Applied Acoustics* 61 (2000) 247–269.
[6] T.R.T. Nightingale, I. Bosmans, Estimating junction attenuation in lightweight construction, *Proceedings of Internoise 2000*, Nice, France, Paper IN2000/342, 2000.
[7] T.R.T. Nightingale, I. Bosmans, Vibration response of lightweight wood frame building elements, *Building Acoustics* 6 (1999) 269–288.
[8] B.M. Gibbs, J.D. Tattersal, Vibrational energy transmission and mode conversion at a corner junction of square section rods, *Journal of Vibration, Acoustics, Stress, and Reliability in Design* 109 (1987) 348–355.
[9] L. Cremer, M. Heckl, E.E. Ungar, *Structure-Borne Sound*, second ed., Springer, Berlin, 1988.

[10] F.J. Fahy, A.D. Mohammed, A study of uncertainty in applications of SEA to coupled beam and plate systems—part I: computational experiments, *Journal of Sound and Vibration* 158 (1992) 45–67.
[11] R.J.M. Craik, J.A. Steel, D.I. Evans, Statistical energy analysis of structure-borne sound transmission at low frequencies, *Journal of Sound and Vibration* 144 (1991) 95–107.
[12] K.H. Heron, Predictive SEA using line wave impedances, *IUTAM Symposium on Statistical Energy Analysis*, Kluwer Academic Publishers, Dordrecht, 1997.